Reports

Effect of aging on horizontal smooth pursuit.

JAMES A. SHARPE AND TREVOR O. SYLVESTER.

Quantitative infrared oculographic study of horizontal pursuit in young and elderly normal subjects showed significantly lower smooth pursuit velocities in the elderly when tracking triangular waveform targets of 20° amplitude at velocities of 10°/sec and over. Latencies for initiation of smooth eye movements were significantly prolonged in older subjects. The reduced velocity responses of the pursuit system indicate that the diagnosis of abnormal pursuit must be qualified by the age of the patient. Smooth pursuit is an age-dependent motor system.

Smooth pursuit provides a sensitive parameter of brain function. Defective pursuit, evidenced clinically by saccadic tracking of slowly moving targets, is a frequent sign of cerebral, cerebellar, and brain stem disease. The smooth pursuit system can be quantitated by measurement of its gain, the ratio of smooth eye movement (SEM) velocity to target velocity.

Restriction of upward gaze and convergence illustrate effects of senescence on ocular motor function. This study of smooth pursuit in normal subjects, young and elderly, determines the effect of aging on horizontal pursuit.

Methods. Fifteen young volunteers, 19 to 32 years old (mean age 23; eight women, seven men), and 10 elderly volunteers, 65 to 77 years old (mean age 72; seven women, three men), served as subjects. Mental status and neuro-ophthalmologic examination results were considered normal for the age of each subject. None had a history of neurologic disease. No subject had received sedative, hypnotic, or other psychoactive drugs within a week preceding testing. Horizontal eye movements were recorded by infrared reflection devices mounted on spectacle frames. Subjects were seated with their heads stabilized by chin, brow, and occipital supports. Their visual acuities were corrected to 20/40 or better in the eye used to measure pursuit. Eye position signals were D.C.-coupled to an ink-jet writing rectolinear polygraph. The full system bandwidth was 250 Hz. All recordings were made within ±10° of the primary position. SEM velocities were determined by electronic differentiation of the eye position signals. We could interpret intersaccadic SEM velocities to a resolution of 1.3°/sec by inspection of the recordings.

The pursuit target was a 6328 Å laser, rear-projected on a featureless screen 0.82 meters from the subjects. The target subtended a visual angle of 0.25° and had a luminance 4.1 log units above foveal threshold. It was driven by triangular waveforms in predictable ramps of 20° amplitude at nine frequencies from 0.125 to 2.5 Hz corresponding to ramp velocities of 5°, 10°, 20°, 30°, 40°, 50°, 60°, 80°, and 100°/sec. Subjects were instructed to follow the light, attempting to keep

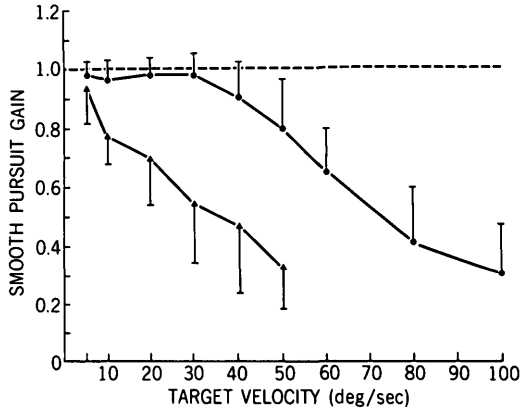

Fig. 1. Horizontal smooth pursuit gain (eye velocity/target velocity) of 15 young (•) and 10 elderly (▲) subjects. Means and standard deviations.

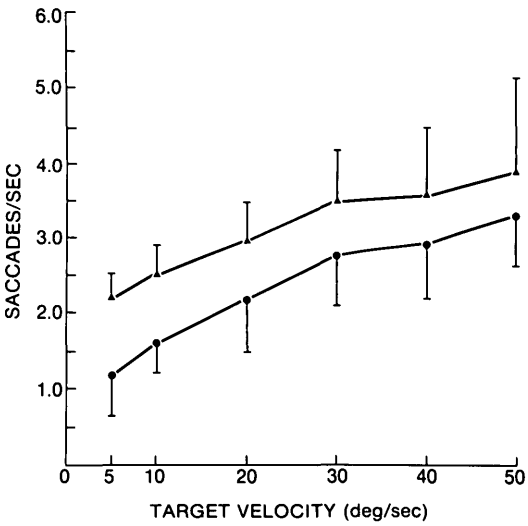

Fig. 2. Saccadic frequency of 10 elderly (▲) and 15 young (•) subjects plotted against target velocity. Means and standard deviations.

0146-0404/78/0517-0465$00.40/0

Table I. Mean SEM velocities and highest individual subject values

	Target velocity (degrees/sec)					
	5	*10*	*20*	*30*	*40*	*50*
Young subjects:						
Group mean ± S.D.	4.9 ± 0.2	9.6 ± 0.7	19.6 ± 1.2	29.3 ± 2.4	36.0 ± 5.2	39.4 ± 9.0
Maximum individual subject value	5.8	12.2	25.0	43.0	47.5	56.0
Elderly subjects:						
Group mean ± S.D.	4.7 ± 0.6	8.7 ± 0.9	13.8 ± 3.2	16.2 ± 6.3	18.4 ± 9.2	16.0 ± 7.5
Maximum individual subject value	5.6	11.3	22.5	32.5	42.5	30.0

Table II. Smooth pursuit latencies (mean ± S.D.)

	Target velocity (degrees/sec)		
	5	*10*	*20*
Young subjects:			
Latency (msec)	131 ± 23	138 ± 21	134 ± 34
No. of subjects	10	12	11
Elderly subjects:			
Latency (msec)	176 ± 33	183 ± 49	169 ± 37
No. of subjects	5	5	8

their eyes on it at all times. Attentive tracking was encouraged by frequent vigorous verbal stimulation.

For each subject the 15 highest SEM velocities from series of over 30 ramps were measured to obtain mean pursuit velocity at each target frequency. Group data for targets over 50°/sec were not obtained in the elderly, since an insufficient number of SEM's occurred in individual subjects and tracking consisted of saccades. Latencies from the onset of target motion to the beginning of smooth pursuit were obtained in some subjects for randomly presented single ramps (N = 5) at velocities up to 20°/sec. The mean number of saccades per second was calculated from the same velocity records used to measure SEM velocities. We determined the frequency of saccades having peak velocities over 15° to 20°/sec, corresponeing to saccadic amplitudes of approximately 10 to 15 minutes of arc, which were not visible on the eye position signals at the recording calibrations used.

Results. The ratios of mean SEM velocity to target velocity (gain) are shown in Fig. 1. In the group of young subjects, gain exceeded 0.96 at target velocities up to 30°/sec, but in the elderly group, the highest mean gain was 0.94 when tracking a 5°/sec target. There was no significant difference between leftward and rightward pursuit in any subject. SEM velocities were equal in men and women. The age group differences were statistically significant at target velocities of 10°/sec and over (t tests, $p < 0.02$ at 10°/sec and $p < 0.001$ at 20°/sec and over). Single maximum SEM values exceeding slow target velocities occurred in subjects in both age groups. The highest single SEM velocity in any individual subject in the young group was 75°/sec at a target velocity of 80°/sec. One elderly subject made a SEM of 43°/sec at a target speed of 40°/sec (Table I). Smooth pursuit latencies were significantly prolonged in elderly subjects ($p < 0.05$; Table II).

With increasing target speed, tracking was performed by increments of saccadic amplitude and frequency. The number of saccades per second was greater in the elderly group (Fig. 2; $p < 0.05$ at 40°/sec and under).

Discussion. This quantitative study of the smooth pursuit system indicates that its gain declines in old age. Reduction in SEM velocities during pursuit of fixed-amplitude triangular target sequences does not specify a decreased steady-state velocity range of the pursuit system in the elderly, since a reduced frequency response would also limit its output. Eye position and velocity records in elderly subjects showed that the reduced SEM velocities reached optimal steady-state values before the target and eyes changed direction when tracking these 20° targets at frequencies up to 1.25 Hz (50°/sec). The ratios of SEM velocity to target velocity in our young group are similar to the smooth pursuit gains described by Zee et al.[1] for normal subjects tracking triangular waveform targets of the same amplitude.

Although the goal of the smooth pursuit system is foveation of a moving target by matching eye velocity to target velocity, Puckett and Steinman[2] reported an optimal mean pursuit gain of 0.87 for an experienced subject tracking ramps moving at only 1°/sec. The higher SEM values in our subjects may be attributed to methodologic differ-

60	80	100
38.4 ± 10.0 61.0	32.2 ± 15.2 75.0	29.1 ± 18.0 70.0
— 25.0	— 15.0	— —

ences. We employed predictable target sequences to enhance tracking performance. The 20° target amplitudes, being about seven times larger than in the Puckett and Steinman study, afforded more time for velocity matching. Moreover, our data do not exclude any contribution of miniature saccades to the SEM values. We used a large bright target to reduce possible effects of any senile macular degeneration on retinal feedback, and a 633 nm laser source which the aging lens transmits better than shorter wavelengths.[3] In order to minimize impairment of pursuit from fatigue or inattention, mean SEM velocities were derived from optimal values in both age groups.

Latencies for initiation of SEM were significantly prolonged in elderly subjects. Mean pursuit latencies of our young subjects were comparable to values obtained by Robinson[4] in three subjects. The latencies were not dependent on target velocity (stimulus amplitude). We did not determine the visual efficacy of tracking or the ability of catch-up saccades to compensate for impaired smooth pursuit in old age by improving mean eye position relative to the target. Reduced SEM responses in the elderly may be expected to impair their acuity for moving objects; dynamic visual acuity falls with increasing target velocity, and the decline correlates with failure of the pursuit system to correct retinal errors.[5]

As SEM velocities fail to match faster targets, increasing retinal position errors produce increments of saccadic amplitude[4] and frequency.[5] Since the clinical detection of impaired smooth pursuit is influenced by estimates of the number of saccades occurring during tracking, we determined saccadic frequency in both age groups (Fig. 2). A report[6] of tracking performance based upon visual estimation of the irregularity of eye position recordings, without measurement of pursuit velocity or saccadic frequency, described better tracking in young adults than in subjects over age 50 and better tracking in men than in women. We found no significant difference in SEM velocity or saccadic frequency between the sexes. We observed that our clinical judgment of the number and amplitude of saccades generally provided a reliable criterion for detecting the abnormal pursuit quantitated by low SEM velocities in older subjects.

The low smooth pursuit gain identified in the elderly can be explained by nervous system degeneration accruing with age. Neither nuclear nor supranuclear brain stem involvement can be implicated in view of reports of normal microscopic structure of the abducens nucleus[7] and brain stem tegmentum[8] in senescence. Cerebral cortical atrophy, loss of cerebellar Purkinje cells,[9] and degeneration of extraocular muscles[10] are senile changes that may be responsible, individually or in concert. Our results indicate that the diagnosis of abnormal horizontal pursuit in neuro-ophthalmic disease must be qualified by the age of the patient. Smooth pursuit is an age-dependent motor system.

From the Neuro-ophthalmology Unit, Division of Neurology, Toronto Western Hospital, University of Toronto, Toronto, Ont., Canada. This study was supported by Medical Research Council of Canada grants ME 5509 and MA 5404. Submitted for publication Aug. 29, 1977. Reprint requests: James A. Sharpe, M.D., Toronto Western Hospital, 399 Bathurst St., Toronto, Ont. M5T 2S8, Canada.

Key words: eye movements, smooth eye movements, smooth pursuit, saccades, eye movement velocity, eye movement recording, smooth pursuit gain, aging

REFERENCES

1. Zee, D. S., Yee, R. D., Cogan, D. G., Robinson, D. A., et al.: Ocular motor abnormalities in hereditary cerebellar ataxia, Brain 99:207, 1976.
2. Puckett, J. D. W., and Steinman, R. M.: Tracking eye movements with and without saccadic correction, Vision Res. 9:695, 1969.
3. Said, F. S., and Weale, R. A.: The variation with age of the spectral transmissivity of the living human crystalline lens, Gerontologica 3:213, 1959.
4. Robinson, D. A.: The mechanics of human smooth pursuit eye movement, J. Physiol. 180:569, 1965.
5. Brown, B.: Dynamic visual acuity, eye movements and peripheral acuity for moving targets, Vision Res. 12:305, 1972.
6. Kuechenmeister, C. A., Linton, P. H., Mueller, T. V., et al.: Eye tracking in relation to age, sex illness, Arch. Gen. Psychiat. 34:578, 1977.
7. Vijayashankar, N., and Brody, H.: A study of aging in the human abducens nucleus, J. Comp. Neurol. 173:433, 1977.

8. Ishii, T.: Distribution of Alzheimer's neurofibrillary changes in the brain stem and hypothalamus of senile dementia, Acta Neuropathol. 6:181, 1966.
9. Hall, T. C., Miller, A. K. H., and Corsellus, J. A. N.: Variations in the human Purkinje cell population according to age and sex, Neuropathol. Appl. Neurobiol. 1:267, 1975.
10. Miller, J. E.: Aging changes in extraocular muscle. *In* Lennerstrand, G., and Bach-y-Rita, P., editors: Basic Mechanisms of Ocular Motility and their Clinical Implications, Oxford, 1975, Pergamon Press, p. 47.

Ocular retardation (or) in the mouse.

RICHARD M. ROBB, JERRY SILVER, AND RICHARD T. SULLIVAN.

The ocular retardation (or) mutation in mice has been studied morphologically in serial 1 μ sections. This recessively inherited, fully penetrant mutation is characterized by an early arrest of retinal development, aplasia of the optic nerve, cataractous degeneration of the lens, and microphthalmia. We describe early alterations of normally occurring morphogenetic cell death in the optic cup and aberrations of optic fissure formation which appear to precede the arrest of retinal and optic nerve development. The subsequent disappearance of central retinal vessels and cataract formation are interpreted as secondary phenomena.

Ocular retardation (or) is a recessive gene mutation in the mouse which causes microphthalmia associated with a progressive dissolution of the retina, aplasia of the optic nerve, and cataractous degeneration of the lens. The mutation, which has complete penetrance in the homozygous state, was initially described in 1962 by Truslove,[1] who suggested that failure of development of the retinal blood supply led to the eventual retrogressive changes in the globe. More recently at the Jackson Laboratory a mutation with similar pathological features arose spontaneously in the 129/Sv-Sl^{J}CP colony of mice. Tests for allelism revealed that this new mutation was allelic with ocular retardation, and the new mutant was assigned the symbol or^{J}.[2] Theiler et al.[3] in 1976 noted in the or^{J} embryo an absence of normally occurring cell death in the eye cup stage of development. Silver and Hughes[4] previously had proposed such an absence of morphogenetic cell death as a causative factor in the production of anophthalmia in a different strain of mice. Because of our interest in the early morphogenesis of the eye, we undertook a further morphological study of the or^{J} mutation in order to define as precisely as possible the earliest aberrations of ocular development.

Materials and methods. Mutant mice of the 129/Sv-Sl^{J}CP strain, homozygous for the ocular retardation gene, were compared to normal animals from the same strain. Timed embryos were obtained by the vaginal plug method, the time of conception being taken as midnight preceding the morning on which a plug was found. Pregnant animals were killed on various gestational days with pentobarbital. The embryos were removed from the uterus in 0.15M phosphate buffer (pH 7.2), and the heads were fixed overnight at room temperature in a combination of 0.5% glutaraldehyde and 2% formaldehyde solution. The material was postfixed in 1% OsO_4 at 4°C for 2 hr and was then processed through graded alcohols and propylene oxide to be embedded in Epon. The eyes of postnatal animals were fixed and embedded in similar fashion. For each gestational and postnatal stage, 1 μ serial sections were cut through the eye in each of three planes: sagittal, coronal, and frontal. The sections were stained with toluidine blue for light microscopy.

Results. At 10.5 days of gestation the optic vesicle of normal mice is well into the initial stages of invagination to form the optic cup. This cup surrounds the lens pit from the surface ectoderm on all sides except the ventral side, where the most distal or retinal portion of the optic fissure is located. This fissure allows mesenchymal cells access to the interior of the optic cup, where a vascular network is eventually established. The over-all appearance of mutant eyes at 10.5 days was similar to that of normal eyes. The volume of the eye and the extent of invagination to form the retinal fissure were comparable. In one respect, however, mutant eyes differed from normal eyes at 10.5 days. In the mutant retina there was no evidence of cell death, whereas zones of cell necrosis were present in the normal retina and in both mutant and normal retinal pigmented epithelium and lens. The same striking absence of necrotic foci in the developing retina of mutant animals was apparent at 11.0 and 11.5 days of gestation (Fig. 1, *A*). This was in contrast to the increasing numbers of necrotic cells in normal animals, located especially within the base of the retina just dorsal to the area of the retinal fissure (Fig. 1, *B*). The normal pattern of cell death during these and other stages of eye development has been described more fully by Silver and Hughes[5] in 1973.

At day 11 abundant vascularization of the interior of the optic cup by way of the retinal portion of the optic fissure was present in normal and mutant eyes (Fig. 1). The more proximal extent of the optic fissure at the base of the retina and in the

0146-0404/78/0517-0468$00.60/0

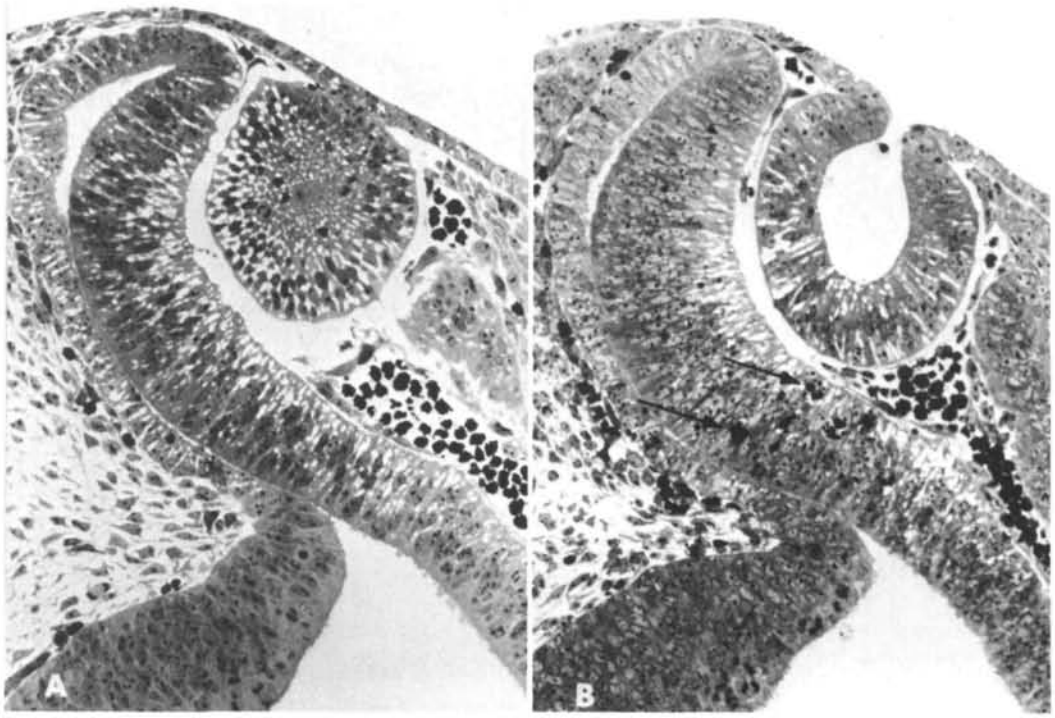

Fig. 1. Sagittal sections of eyes at 11.0 days' gestation. **A,** Eye of or^{J} mutant. Vessels have entered optic cup through retinal portion of optic fissure. There are no necrotic foci in the retinal rudiment. The lens pit is forming normally. (×235.) **B,** Normal eye. Note zones of necrosis in dorsal retina (arrows). Vascularized mesenchyme has entered optic cup through retinal portion of optic fissure. (×235.)

optic stalk was just becoming apparent at 11 days, but by 11.5 days it was well established in the optic stalk of normal animals (Fig. 2, *A*). In mutant animals this optic stalk fissure was delayed in its formation and remained abnormal throughout development (Fig. 2, *B*). At 11.5 days only a small intrusion of neuroectodermal cells into the stalk lumen was evident. Vascularized mesenchyme was only sparsely represented in this ventral intrusion in the mutants, whereas in normal animals the vessels which had originally entered the eye through the retinal portion of the optic fissure eventually came to course well back into the optic stalk fissure (Fig. 2).

By 12.5 days of gestation other major differences were apparent between normal and mutant eyes. Retinal ganglion cells had differentiated and had sent axons back along the optic stalk in normal animals, whereas in or^{J} animals no evidence of ganglion cell differentiation was apparent. In the mutant animals there now were large numbers of degenerating cells in the retina and optic stalk, especially in the ventral region adjacent to the optic fissure (Fig. 3). These necrotic foci were in excess of the number seen at this time in normal animals. The edges of the fissure were partially overlapping and redundant, but they were closely approximated and appeared to be closing. Some blood vessels still entered the eye through the posterior extent of the optic fissure. The mutant eye appeared slightly smaller than its normal control, especially in its more ventral portions.

By 14.5 days of gestation, the eye and optic nerve of normal animals had steadily increased in volume as greater numbers of ganglion cells differentiated and sent axons back toward the brain (Fig. 4, *A*). In the or^{J} mutant by day 15 all remaining fissures in the retina and optic stalk had closed completely. A substantial retinal neuroblastic layer was present, but it was difficult to distinguish ganglion cells. Although there was some indication of nerve fiber formation at the inner surface of the retina, its development was meager, and no axons exited from the eye (Fig. 4, *B*). In the absence of an optic nerve, the optic stalk regressed and became a slender cord of cells. The opening in the posterior retina for passage of the hyaloid vessels was completely closed at this stage. Blood vessels,

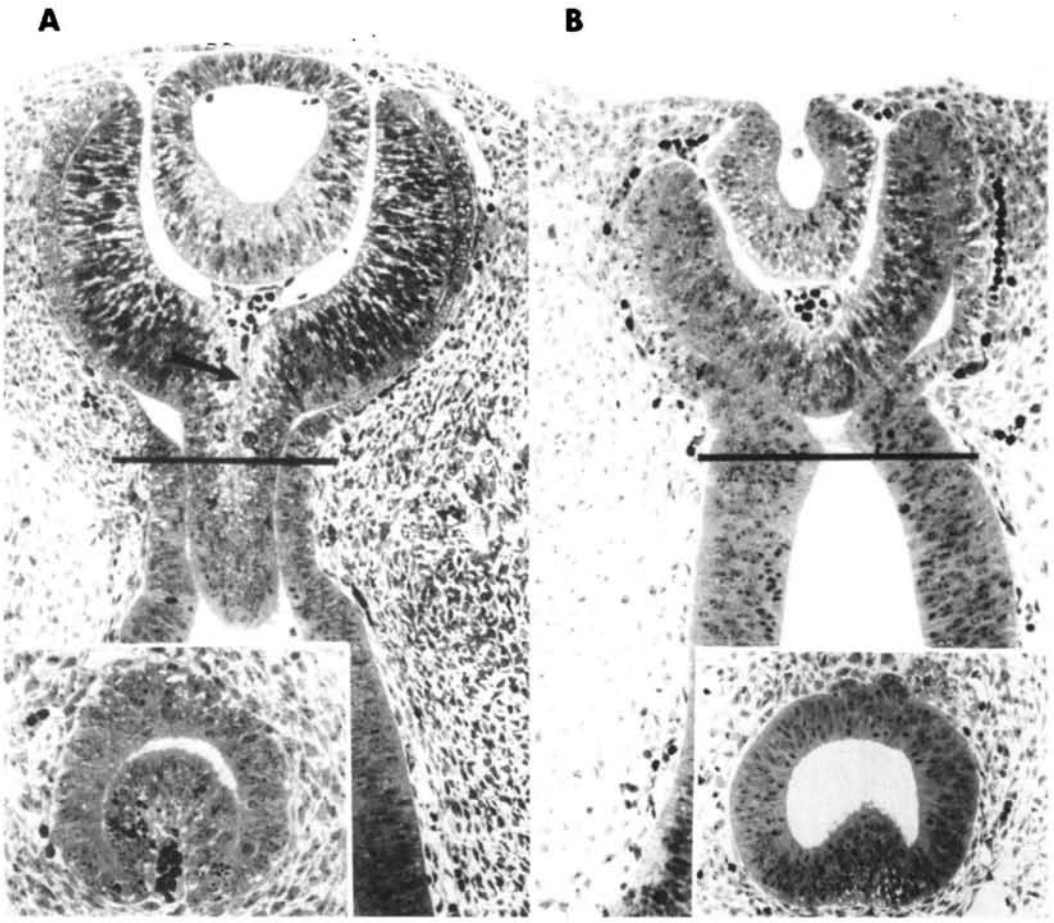

Fig. 2. Eyes at 11.5 days' gestation. **A**, Normal eye. The optic stalk fissure is readily apparent in this coronal section (arrow). Vascularized mesenchyme is enclosed in the cleft of the optic fissure. (×165.) *Inset:* Cross-section of optic stalk at level indicated by black line. (×210.) **B**, Eye of or^J mutant. The optic stalk fissure is not apparent in this coronal section. (×165.) *Inset:* Cross-section of mutant optic stalk. Only a slight intrusion of neuroectodermal cells has formed on the ventral surface of the stalk where the optic fissure would normally exist. (×135.)

nevertheless, persisted within the secondary eye chamber, in part due to branches from the annular vessels which entered over the anterior rim of the optic cup. At this time the amount of cell death was much diminished in both normal and mutant retinas.

At 16.5 and 18.5 days of gestation further retrogressive changes were apparent in the mutant eye. The retina failed to differentiate into recognizable layers and gradually became thinner. Vitreous did not develop, although blood vessels remained on the adjacent surfaces of retina and lens. The lens itself, which had formed primitive lens fibers and a capsule, now developed vacuoles and lost its ordered fibrillar appearance. Although a clear cornea developed, the anterior margin of the optic cup did not mature into a recognizable iris and ciliary body. Postnatally the lens became cataractous, liquefied, and shrunken. The retina further degenerated into a layer 2 to 4 cells thick. The optic stalk disappeared except for a few cells at the posterior pole of the globe. The eye remained smaller than normal, shrunken behind closed lids, and apparently sightless.

Discussion. The presence of early abnormalities of cell death in the eye rudiment of or^J mice suggests that the pathophysiology of the mutation is different from the retinal vascular insufficiency proposed by Truslove.[1] Our own observations indicate that the optic cup is well vascularized

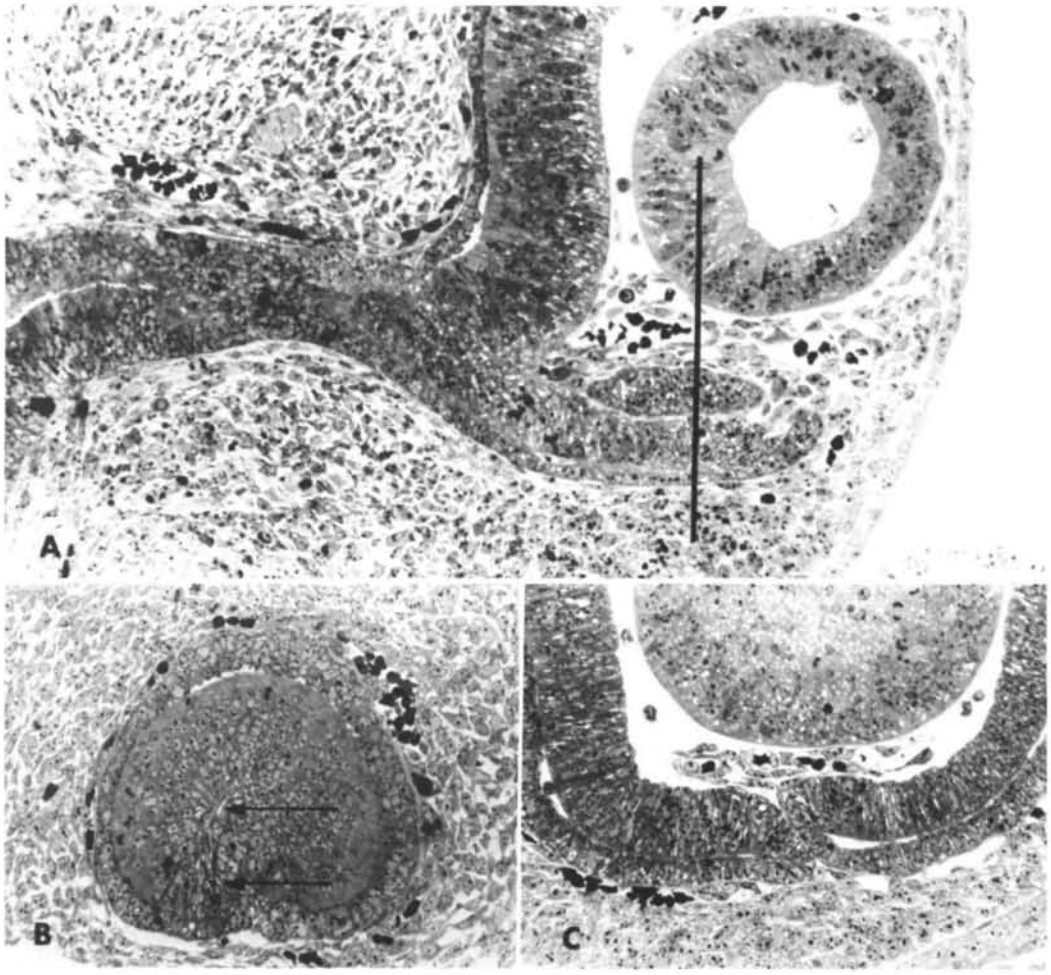

Fig. 3. Eye of or^{J} mutant at 12.5 days' gestation. **A.** Sagittal section. No axons are apparent in the developing retina, but zones of necrosis have appeared, especially in the ventral region of the optic cup. (×260.) **B,** Cross-section of optic stalk just behind globe, showing fissure (arrows) which is closed and curvilinear in shape. There are mitotic activity near the ventricular surface and cell necrosis adjacent to the fissure. (×220.) **C.** Frontal section of retinal fissure at level indicated by black line in **A,** showing overlap of the edges of the optic cup. (×220.)

beyond the time of the early morphological aberrations of the mutant. It seems likely that the eventual absence of a central retinal vessel is a secondary phenomenon, as is the absence of an optic nerve.

Theiler et al.[3] recognized the early absence of morphogenetic cell death but interpreted the abnormalities of optic fissure formation as a "plug" which might mechanically obstruct egress of optic nerve fibers or prevent access of a chemotactic factor for the outgrowth of nerve fibers. We are more inclined to interpret the abnormalities of optic fissure formation as a reflection of an underlying cellular defect which first expresses itself as an aberration in the timing of morphogenetic cell death in the optic cup and later becomes manifest as a failure of the retinal precursors to differentiate beyond a rudimentary level. It is not clear what role the optic fissure plays in facilitating the passage of retinal ganglion cell axons back to the central nervous system. Mann[6] and Kuwabara[7] have noted that the optic nerve fibers do not pass through the cleft of the optic stalk fissure itself on their way to the chiasm but rather travel between elongated stalk cells which eventually become the glia of the optic nerve. Therefore a simple plug-

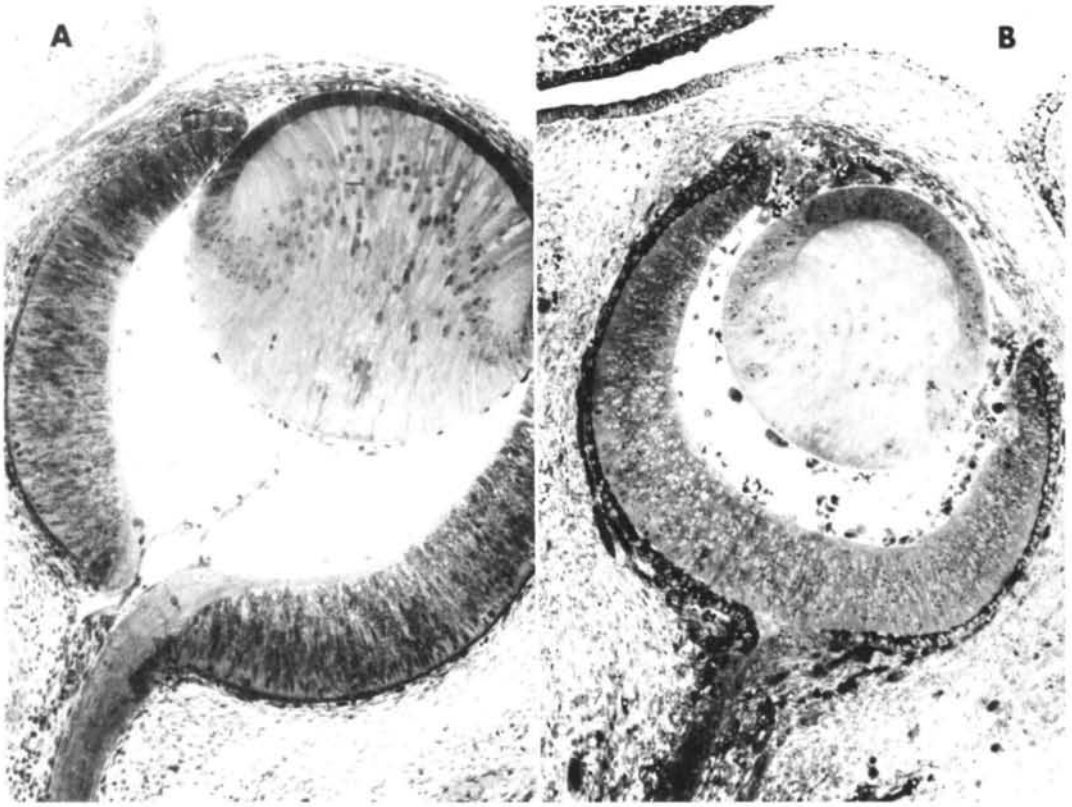

Fig. 4. Sagittal sections of eyes at 14.5 days' gestation. **A**, Normal eye. Axons of ganglion cells exit from the eye in increasing numbers. The hyaloid vessels can be seen reaching forward to the lens. (×160.) **B**, Eye of or^J mutant. The retinal fissure has closed, and hyaloid vessels are not apparent. The optic cup remains heavily vascularized, however, and there is a substantial retinal neuroblastic layer. No retinal ganglion cell axons exit from the eye. The optic stalk is reduced in size. (×160.)

ging of the optic fissure might not affect the passage of nerve fibers.

The increase in zones of necrosis in the mutant retina and optic stalk on embryonic day 12.5 is as remarkable as is the earlier lack of morphogenetic cell death in these same areas. The burst of cell death coincides with closure of the retinal portion of the optic fissure anteriorly. Posteriorly it occurs along the swollen, overlapping edges of the optic stalk fissure. It may be that this late cell necrosis, occurring in areas which are actively changing shape, represents an effort of the eye to recover from its already aberrant pattern of development.

From the Departments of Ophthalmology, Children's Hospital Medical Center, and Harvard Medical School, Boston, Mass. This work was supported in part by a U.S. Public Health Service Mental Retardation Research Program Grant 2P30-HD 06276 from The National Institute of Child Health and Human Development. Submitted for publication Sept. 16, 1977. Reprint requests: Dr. Richard M. Robb, Department of Ophthalmology, Children's Hospital Medical Center, 300 Longwood Ave., Boston, Mass. 02115.

Key words: microphthalmia, aplasia of optic nerve, genetic mutation, morphogenetic cell death, optic fissure formation, abnormal retinal development

REFERENCES

1. Truslove, G. M.: A gene causing ocular retardation in the mouse, J. Embryol. Exp. Morphol. **10**:652, 1962.
2. Varnum, D. S., and Nadeau, J. H.: Mouse News Letter 53:35, 1975.
3. Theiler, K., Varnum, D. S., Nadeau, J. H., Stevens, L. C., and Cagianut, B.: A new allele of ocular retardation: early development and morphogenetic cell death, Anat. Embryol. **150**:85, 1976.
4. Silver, J., and Hughes, A. F. W.: The relationship between morphogenetic cell death and the development of congenital anophthalmia, J. Comp. Neurol. **157**:281, 1974.

5. Silver, J., and Hughes, A. F. W.: The role of cell death during morphogenesis of the mammalian eye, J. Morphol. **140**:159, 1973.
6. Mann, Ida: The Development of the Human Eye, ed. 3, New York, 1969, Grune & Stratton, Inc., p. 138ff.
7. Kuwabara, T.: Development of the optic nerve of the rat, INVEST. OPHTHALMOL. **14**:732, 1975.

Iontophoresis of vidarabine monophosphate into rabbit eyes.

JAMES M. HILL, NO-HEE PARK,* LOUIS P. GANGAROSA, DAVID S. HULL, CAROL L. TUGGLE, KAREN BOWMAN, AND KEITH GREEN.

In order to investigate the efficacy of iontophoresis for increasing the penetration of vidarabine monophosphate into the eye, tritium-labeled vidarabine monophosphate was applied to rabbit eyes by topical and iontophoretic application, and the penetration of the compound into the eye, and its subsequent metabolism, were studied. At 20 min after treatment, the ratios of radioactivity for cathodal iontophoresis compared to topical application alone were cornea 8.6, aqueous humor 4.8, and iris 2.4; for 60 min the ratios were cornea 12.2, aqueous humor 17.5, and iris 2.5. In addition, the acid-soluble components were extracted from the cornea and aqueous humor. Vidarabine monophosphate, vidarabine, hypoxanthine arabinoside, adenosine, hypoxanthine, and adenine from the acid-soluble fraction were separated by thin-layer chromatography. The amount of vidarabine monophosphate and vidarabine in the cornea and aqueous humor from the iontophoretically treated group was six to 15 times higher than from the group that received topical application of the drug. It was concluded that cathodal iontophoresis resulted in significantly increased penetration of the antiviral drug vidarabine monophosphate into the anterior chamber of the eye. The effects of iontophoresis of vidarabine monophosphate on corneal epithelium, as observed by scanning electron micrographs, were equal to or less than those seen with the topical application of widely used preservatives in ophthalmic preparations.

5-Iodo-2′-deoxyuridine (IDU, idoxuridine) and 9-β-D-arabinofuranosyladenine (Ara-A, vidarabine) are two drugs which can be used topically for the treatment of herpes simplex keratitis. Vidarabine and IDU have several disadvantages as antiviral agents. (1) The water solubility of both drugs is extremely low.[1-4] (2) They are rapidly metabolized to less effective or inactive compounds.[1-4] (3) When applied topically, there is only limited penetration of the drug into the aqueous humor. The use of vidarabine monophosphate (9-β-D-arabinofuranosyl-adenine-5′-monophosphate, Ara-AMP), the phosphorylated form of vidarabine, may eliminate certain of the disadvantages of IDU and vidarabine, since vidarabine monophosphate is a highly charged molecule and its water solubility is high.[1, 4-7] Since Ara-AMP has a charged phosphate group, its transport across the cell membrane is limited. Iontophoresis was used in an attempt to enhance the penetration of this charged molecule into the anterior chamber of the eye.

Methods. Albino rabbits (2.5 kg body weight) were given intravenous urethane (1 to 2 gm/kg body weight) anesthesia. Prior to use in the experiments, the tritiated vidarabine monophosphate (spec. act. 5.0 Ci/mmol) was chromatographed with two different solvent systems,[7, 8] and all the radioactivity present was found to be associated with the vidarabine monophosphate.

An eye cup was inserted with its periphery applied within the limits of the corneal limbus, and 0.7 ml of a 0.1% solution of vidarabine monophosphate (containing 5 μCi of tritiated vidarabine monophosphate) was applied inside the cup for 4 min of topical application. For cathodal (−) iontophoresis, the cathode was in contact with the drug solution, the return electrode (anode) was connected to the shaved right forelimb of the rabbit, and 0.5 mAmp of current was applied for 4 min. Immediately after completion of topical or iontophoretic administration of vidarabine monophosphate, the eyes were washed with Ringer's solution. After either 20 or 60 min, an anterior chamber paracentesis was performed to obtain 0.15 ml of aqueous humor. After rewashing of the corneal surface, the cornea, iris, and lens were removed. These eye tissues were weighed and homogenized with a polytron in 0.5N $HClO_4$ (PCA) for preparation of the acid-soluble fraction. The aqueous humor was treated with 0.5N PCA. After centrifugation, the supernatant, designated as acid-soluble fraction, was collected, neutralized with KOH, and lyophilized. Total radioactivity was determined from an aliquot of each tissue sample. Also the radioactivities of the contralateral eye and blood were determined. From the neutralized and lyophilized acid-soluble fraction, vidarabine monophosphate, vidarabine, hypoxanthine arabinoside (Ara-Hx, 9-β-D-arabino-furanosylhypoxanthine), adenine, hypoxanthine (Hx), and adenosine (Ado) were separated by thin-layer chromatography.[8] An aliquot of the lyophilized sample was spotted on a 0.5 mm silica gel GF 254 (Brinkman chromatographic glass plate). Since the amounts of labeled compounds were so small, nonlabeled vidarabine monophosphate, vidarabine, adenine, Ara-Hx, Ado, and Hx were applied at the origin. The plates were developed with the lower phase of a chloroform-containing solvent prepared

0146-0404/78/0517-0473$00.40/0

Table I. Total radioactivity in acid-soluble fraction of rabbit eye after administration of tritiated vidarabine monophosphate

Treatment	*Min*	*Total radioactivity (dpm ± S.E.)*			
		Cornea	*Aqueous humor*	*Iris*	*Lens*
Topical application	20	9,262 ± 3,477	2,344 ± 850	240 ± 33	00
	60	5,206 ± 1,543	906 ± 443	250 ± 41	00
Cathodal (−) iontophoresis	20	79,571 ± 10,211*	11,303 ± 1,466*	332 ± 13*	199 ± 12*
	60	63,711 ± 3,923†	15,697 ± 2,899†	618 ± 42†	644 ± 273†

Each group contains data from 4 eyes.
*Significantly different ($p < 0.01$) from topical application (20 min) (t test).
†Significantly different ($p < 0.01$) from topical application (60 min) (t test).

Table II. Amount of vidarabine monophosphate and its metabolites in acid-soluble fraction of rabbit cornea after topical or iontophoretic administration

Treatment	*Min*	*Concentration (ng/100 mg wet weight ± S.E.)*				
		Vidarabine monophosphate	*Vidarabine*	*Ara-Hx*	*Adenine*	*Hx and Ado*
Topical application	20	110 ± 29	130 ± 16	150 ± 24	90 ± 11	240 ± 5
	60	50 ± 2	50 ± 15	80 ± 5	50 ± 7	90 ± 2
Cathodal (−) iontophoresis	20	1,560 ± 317*	880 ± 275*	1,640 ± 317*	1,100 ± 166*	1,650 ± 292*
	60	400 ± 54†	190 ± 10†	370 ± 68†	480 ± 9†	410 ± 50†

Each value is a mean of 4 corneas. The concentrations of vidarabine monophosphate and its metabolites were calculated from the radioactivity determined after chromatography and the specific activity of the tritiated vidarabine monophosphate (5 μCi/700 μg).
*Significantly different ($p < 0.01$) from topical application (20 min) (t test).
†Significantly different ($p < 0.01$) from topical application (60 min) (t test).

Table III. Amount of vidarabine monophosphate and its metabolites in aqueous humor of rabbit eye after topical or iontophoretic administration

Treatment	*Min*	*Concentration (ng/100 μl of aqueous humor ± S.E.)*				
		Vidarabine monophosphate	*Vidarabine*	*Ara-Hx*	*Adenine*	*Hx and Ado*
Topical application	20	5 ± 1.6	9 ± 3.6	29 ± 6.6	8 ± 1.7	2 ± 0.9
	60	4 ± 1.1	11 ± 1.7	45 ± 4.9	10 ± 2.0	2 ± 1.2
Cathodal (−) iontophoresis	20	44 ± 4.2*	38 ± 3.5*	87 ± 2.0*	23 ± 2.0*	20 ± 2.3*
	60	45 ± 7.7†	28 ± 2.7†	195 ± 33.2†	25 ± 4.7†	10 ± 1.9†

The concentrations of vidarabine monophosphate and its metabolites were calculated from the radioactivity determined after chromatography and the specific activity of the tritiated vidarabine monophosphate (5 μCi/700 μg).
*Significantly different ($p < 0.01$) from topical application (20 min) (t test).
†Significantly different ($p < 0.01$) from topical application (60 min) (t test).

by mixing chloroform, methanol, and 3% acetic acid (3:2:1). The well-defined spots of vidarabine monophosphate, vidarabine, Ara-Hx, adenine, Hx, and Ado were visualized under ultraviolet (UV) light and had R_f values of 0.00, 0.30, 0.20, 0.50, 0.42, and 0.42, respectively. The spots were scraped into vials, and the radioactivity was determined.

Results. Table I shows the total radioactivity present in the cornea, aqueous humor, iris, and lens 20 and 60 min after treatment. In all these eye tissues, the highest level of radioactivity was obtained after cathodal iontophoresis of tritiated vidarabine monophosphate. At 20 min after treatment, the ratios of total radioactivity for cathodal iontophoresis compared to topical application were cornea 8.6, aqueous humor 4.8, iris 2.4; at 60 min after treatment the ratios were cornea 12.2, aqueous humor 17.5, and iris 2.5. No radioactivity was detected in the lenses of eyes receiving topical application of tritiated vidarabine monophosphate. In eyes receiving cathodal iontophoresis of the drug, a significant level of radioactivity was present in the lens at 20 and 60 min after treatment. In

Fig. 1. Scanning electron micrograph of corneal epithelial surface 4 min after cathodal iontophoresis of vidarabine monophosphate. A few superficial cells are damaged and some are desquamating. (×200.)

the aqueous humor, iris, and lens, the radioactivity was higher 60 min after iontophoresis than at 20 min, but in the cornea the levels were lower at 60 min when compared to levels at 20 minutes. No radioactivity was detected in the contralateral eye or the blood.

Tables II and III show the amounts of vidarabine monophosphate, vidarabine, Ara-Hx, adenine, Hx, and Ado present in the cornea and aqueous humor 20 and 60 min after treatment. Cathodal iontophoresis of tritiated vidarabine monophosphate provides the highest concentrations of vidarabine monophosphate and its metabolites in the cornea and aqueous humor. In Table II note that the levels of tritiated vidarabine monophosphate and its metabolites in the cornea are lower at 60 min after application than at 20 min. However, in the aqueous humor (Table III), the levels of the drug and metabolites are generally about the same at 60 and 20 min after drug administration, with the exception of Ara-Hx which is significantly increased 60 min after drug administration.

Slit-lamp examination after fluorescein staining of the corneal surface revealed no difference in the staining of corneas treated by either the iontophoretic or topical application of vidarabine monophosphate. The corneal epithelium was examined by scanning electronmicroscopy (SEM). Immediately after topical or iontophoretic application of Ara-AMP, SEM of the cornea showed a very small amount of surface pitting, with limited exposure of cells underlying the superficial epithelium. Fig. 1 shows the scanning electron micrograph of the cornea after iontophoretic application of vidarabine monophosphate.

Discussion. Cathodal iontophoresis of Ara-AMP significantly increased its penetration into rabbit eyes as compared to topical application. Furthermore, iontophoresis resulted in high levels of the antiviral agent deep in the corneal stroma and aqueous humor. This may be of benefit in the treatment of deep stromal herpes keratitis and herpes uveitis. Whether there are potential dangers from the high concentrations of antiviral agents in the lens, e.g., cataract formation, is not known and warrants further investigation. Although the ocular penetration of vidarabine monophosphate was greatly enhanced by cathodal iontophoresis, no radioactivity was detected in the blood or contralateral eye. It appears that the tritiated vidarabine monophosphate and its radioactive metabolites do not diffuse into other tissues and are metabolized by known pathways.[1, 4-7] Most of the vidarabine monophosphate is dephosphorylated to vidarabine; the vidarabine can be deaminated to Ara-Hx or cleaved to arabinose and adenine. Although the level of penetration of vidarabine monophosphate is significantly higher for iontophoresis than for topical application, the

metabolic degradation remains the same. In the cornea (Table I and II) vidarabine monophosphate appears to be more rapidly metabolized after topical application compared to iontophoretic application. In the aqueous humor (Table III), the amounts of vidarabine monophosphate and vidarabine are almost the same 20 and 60 min after iontophoretic and topical application. Therefore the catabolism in the aqueous humor must be slower, diffusion from the cornea higher, or some combination of the two in order to maintain the same amount of vidarabine monophosphate and vidarabine for 20 and 60 min.

Erlanger[9] used iontophoresis as a procedure for obtaining high levels of drugs in eye tissues. Although iontophoresis is an uncomplicated, safe, well-documented method for assuring penetration of charged drugs, the technique has not been widely used. Harris[10] has reviewed the uses of iontophoresis in medicine and dentistry and cited the advantages of iontophoresis in drug delivery to surface tissues, giving numerous examples. Iontophoresis offers the advantages of assuring penetration of the drug to the desired site, i.e., corneal stroma and aqueous humor, and is an alternative to topical application, systemic administration, or direct injection into the eye tissue.

The radioactive vidarabine monophosphate was supplied through the courtesy of Drs. T. J. Petrick and A. J. Glazko, Warner Lambert–Parke, Davis & Co., Ann Arbor, Mich. Scanning electron microscopy was performed by Mid-America Microanalysis, Milwaukee, Wisc.

From the Departments of Cell and Molecular Biology, Pharmacology, Oral Biology, Ophthalmology, and Physiology, Medical College of Georgia, Augusta. Supported in part by grants from Parke, Davis & Co. (J. M. H. and N. H. P.), National Eye Institute EY-01413 (K. G.), and NIDR-DE-04917 (J. M. H.). *Present address: Harvard Medical School, Eye Research Institute of Retina Foundation, Boston, Mass. Submitted for publication Sept. 13, 1977. Reprint requests: James M. Hill, Ph.D., Department of Cell and Molecular Biology, Medical College of Georgia, Augusta, Georgia 30901.

Key words: iontophoresis, vidarabine, vidarabine monophosphate, hypoxanthine arabinoside, corneal epithelium, cornea, aqueous humor

REFERENCES

1. Hill, J. M., Gangarosa, L. P., and Park, N. H.: Iontophoretic application of antiviral chemotherapeutic agents, Ann. N. Y. Acad. Sci. **284**:604, 1977.
2. Gangarosa, L. P., Park, N. H., and Hill, J. M.: Iontophoretic assistance of 5-iodo-2′-deoxyuridine penetration into neonatal mouse skin and effects on DNA synthesis, Proc. Soc. Exp. Biol. Med. **154**: 439, 1977.
3. Pavan-Langston, D., Dohlman, C. H., Geary, P. A., and Sulzewski, D.: Intraocular penetration of ARA-A and IDU—therapeutic implications in clinical herpetic uveitis, Am. Acad. Ophthalmol. Otolaryngol. 77:455, 1973.
4. Pavan-Langston, D., Langston, R. H. S., and Geary, P. A.: Prophylaxis and therapy of experimental ocular herpes simplex. Comparison of idoxuridine, adenine arabinoside, and hypoxanthine arabinoside, Arch. Ophthalmol. **92**:417, 1974.
5. Pavan-Langston, D., North, R. D., Geary, P. A., et al.: Intraocular penetration of the soluble antiviral Ara-AMP, Arch. Ophthalmol. 94:1585, 1976.
6. Trobe, J. D., Centifanto, Y., Zam, Z. S., Varnell, E., and Kaufman, H. E.: Anti-herpes activity of adenine arabinoside monophosphate, INVEST. OPHTHALMOL. **15**:196, 1976.
7. Park, N. H., Gangarosa, L. P., and Hill, J. M.: Iontophoretic application of Ara-AMP (9-β-D-arabinofuranosyl adenine 5′-monophosphate) into adult mouse skin., Proc. Soc. Exp. Biol. Med. **156**:326, 1977.
8. Drach, J. C., and Novack, J. M.: Some simple thin-layer chromatographic systems for the separation of purines and purine nucleosides. Anal. Biochem. **52**:633, 1973.
9. Erlanger, G.: Iontophoresis, a scientific and practical tool in ophthalmology, Ophthalmologica **128**: 232, 1954.
10. Harris, R.: Iontophoresis. *In* Licht, S., editor: Therapeutic Electricity and Ultraviolet Radiation, ed. 2, New Haven, Conn., 1967, E. Licht (Publisher), pp. 156-178.

Histochemical demonstration of cyclic guanosine 3′,5′-monophosphate phosphodiesterase activity in retinal photoreceptor outer segments.

RICHARD M. ROBB.

A technique for the histochemical demonstration of cyclic guanosine monophosphate phosphodiesterase in retina is described. Enzyme activity was identified on photoreceptor outer segment lamellae, a finding in agreement with previous biochemical data on isolated outer segment preparations. The distribution of phosphodiesterase activity for cyclic guanosine monophosphate was similar to that found previously in rod outer segments for cyclic adenosine monophosphate, suggesting that the same enzyme may hydrolyze both nucleotides.

The cyclic nucleotide phosphodiesterase which hydrolyzes cyclic adenosine 3′,5′-monophosphate (cyclic AMP) to 5′-adenosine monophosphate has previously been demonstrated on photoreceptor outer segment lamellae by histochemical means.[1] Although a similar enzyme hydrolyzing cyclic

0146-0404/78/0517-0476$00.50/0

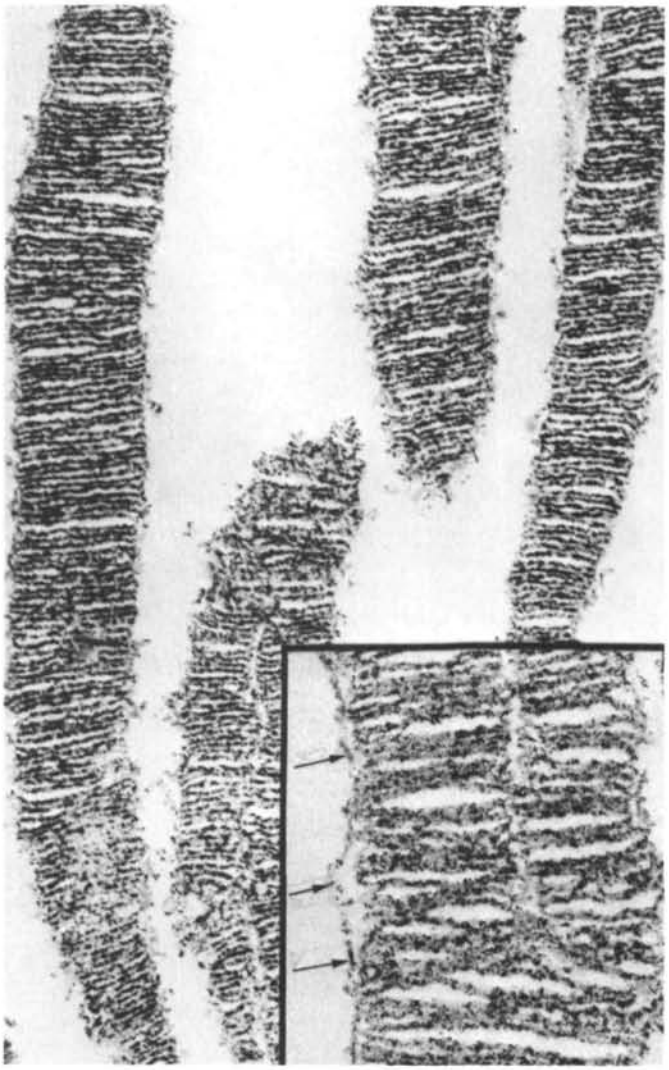

Fig. 1. Photoreceptor outer segments of adult mouse retina incubated with cyclic GMP after brief (3 min) fixation, showing reaction product precipitated on outer segment lamellae. (×21,500.) Inset: Higher-power view of outer segment lamellae and adjacent plasma membrane (arrows), which also contain reaction product. (×40,000.)

guanosine 3′,5′-monophosphate (cyclic GMP) has been identified in photoreceptor outer segment preparations by biochemical techniques,[2] its histochemical demonstration has been inconsistent and uncertain.[1] Since levels of cyclic GMP are high in the retina and since they appear to be light-sensitive,[3] the ultrastructural localization of cyclic GMP phosphodiesterase has been a matter of continuing interest. This report presents a successful method for the histochemical localization of cyclic GMP phosphodiesterase activity in retinal photoreceptor cells.

Method. Normal adult mice of the C57BL/6J inbred strain were used in the study, in anticipation of the desirability of subsequently applying the technique to animals of the same strain with recessively inherited retinal degeneration (rd).[4] The animals were killed with an intraperitoneal injection of pentobarbital and were immediately decapitated. Eyes were removed in room illumination and were immersed in a solution containing 60 mM Tris-maleate buffer (pH 7.4), 2 mM $MgCl_2$, and 0.25M sucrose (TMS buffer). The eyes were opened under an operating microscope,

Invest. Ophthal. Visual Sci.
May 1978

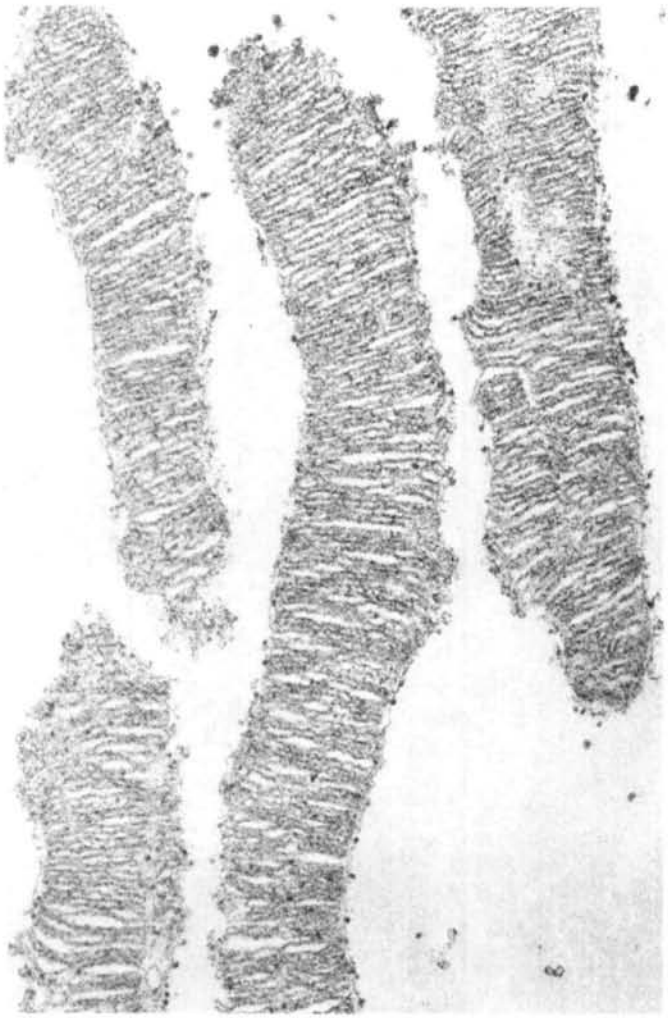

Fig. 2. Photoreceptor outer segments of retina incubated with cyclic GMP plus xanthine inhibitor of phosphodiesterase activity. Reaction product is diminished compared to Fig. 1. (×25,000.)

and the retina was separated gently from the pigmented epithelium. Isolated portions of the retina were then fixed for exactly 3 min with 2% glutaraldehyde in 0.05M cacodylate-nitrate buffer (pH 7.4) containing 0.25M dextrose. The retina was then returned to TMS buffer to be dissected into pieces approximately 0.5 by 1.0 mm.

The pieces of retina were first incubated for 30 min at room temperature in TMS buffer to which was added 5′-nucleotidase in the form of snake venom of *Ancistrodon piscivorus piscivorus*, 1 mg. of dry venom per milliliter.[5] The tissue was then incubated for 30 min at 37° C with slow agitation in TMS buffer containing 2 mM lead nitrate, 5′-nucleotidase (1 mg. of dry venom per milliliter), and 3 mM cyclic GMP. Control experiments were run without the cyclic nucleotide substrate in the second incubation, or with cyclic nucleotide plus 2 mM 1-methyl, 3-isobutyl xanthine, a known inhibitor of phosphodiesterase.[6]

After incubation the retinal tissue was briefly washed in distilled water, dehydrated in graded alcohols, treated with propylene oxide, and embedded in Epon 812. Thin sections were cut, stained with uranyl acetate, and examined with the electron miscroscope.

Results. A lead phosphate precipitate at or near the site of phosphodiesterase activity is the expected result of the above histochemical technique. Such a precipitate was seen along photoreceptor outer segment lamellae (Fig. 1) when tissue fixation times were kept at or below 3 min.

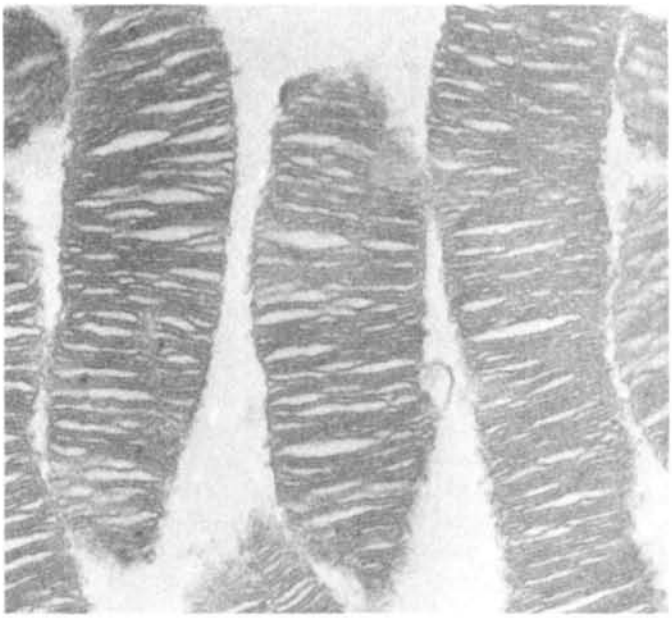

Fig. 3. Photoreceptor outer segments incubated without added cyclic GMP substrate. No reaction product has formed as the result of phosphodiesterase activity. (×24,000.)

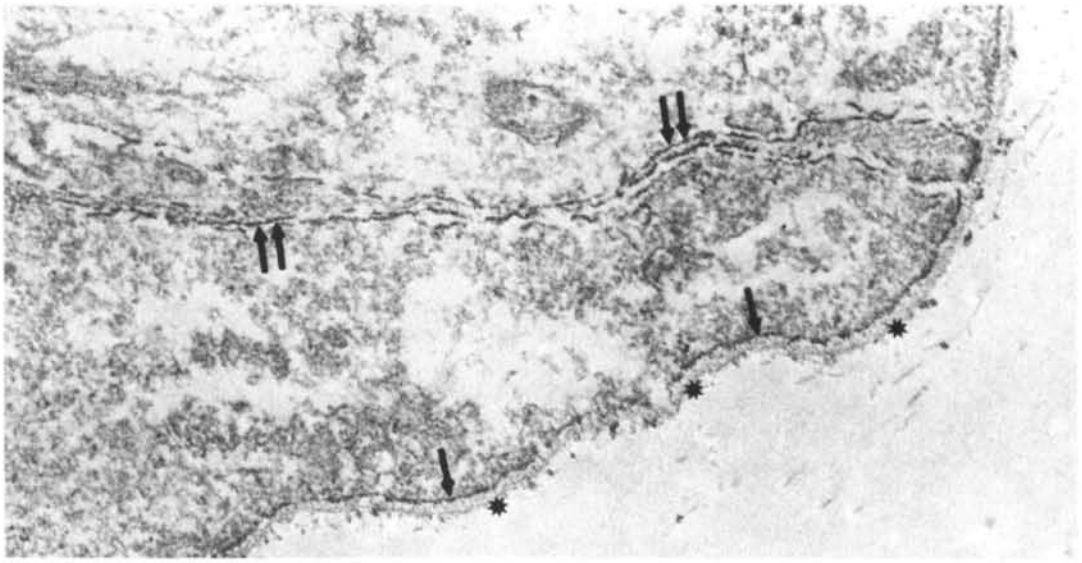

Fig. 4. Inner retina incubated with cyclic GMP, showing reaction product (arrows) beneath basement membrane (asterisks) of Müller cells and on plasma membranes (double arrows) of inner retinal cells. (×30,000.)

With longer fixation times the reaction product became scanty and unpredictable. With fixation times shorter than 3 min the precipitate was heavier, but it tended to obscure the underlying tissue, the morphology of which was already compromised by such a brief period of fixation. The reaction product was much diminished by the addition of a phosphodiesterase inhibitor to the second incubation (Fig. 2). No reaction product at all was seen in experiments in which the cyclic GMP substrate was omitted (Fig. 3). The only other place in the retina at which reaction product was

consistently seen was along the inner retinal surface and along cell membranes of the inner retina (Fig. 4). This localization of enzyme activity had also been noticed in earlier experiments with cyclic AMP as substrate.[1]

Discussion. The previous difficulties in demonstrating cyclic GMP phosphodiesterase activity histochemically in retina appear to have been due to excessive fixation of the tissue. Glutaraldehyde fixation for more than brief periods evidently denatures or alters the enzyme in such a way that it will not react with cyclic GMP. The hydrolysis of cyclic AMP is not as sensitive to fixation, but it too is reduced by prolonged exposure to glutaraldehyde.[1] I have recently used the 3 min fixation time for both cyclic AMP and cyclic GMP and find slightly more reaction product with the former when the conditions of incubation are otherwise similar. The distribution of reaction product on the outer segments is identical with the two substrates, a finding which suggests that one and the same enzyme may be capable of hydrolyzing both cyclic nucleotides.

No precipitate was seen consistently on photoreceptor inner segments, nuclei, or synaptic areas. On the vitreal side of the retina the restriction of precipitate to areas near the retinal surface may reflect limited diffusion of reactants, as discussed previously.[1] The fact that the reaction product was found beneath the basement membrane of the Müller cells rather than on its surface suggests that the precipitate reflects true enzyme activity and not an artifactual deposit.

From the Departments of Ophthalmology, The Children's Hospital Medical Center and Harvard Medical School, Boston, Mass. This work was supported by U. S. Public Health Service grant 5R01 EY01451 from the National Eye Institute, Bethesda, Md. Submitted for publication Feb. 3, 1978. Reprint requests: Dr. Richard M. Robb, Department of Ophthalmology, The Children's Hospital Medical Center, 300 Longwood Ave., Boston, Mass. 02115.

Key words: phosphodiesterase, cyclic GMP, histochemistry, retina, photoreceptor cells

REFERENCES

1. Robb, R. M.: Histochemical evidence of cyclic nucleotide phosphodiesterase in photoreceptor outer segments, INVEST. OPHTHALMOL. 13:740, 1974.
2. Chader, G. F., Johnson, M., Fletcher, R. T., and Bensinger, R. E.: Cyclic nucleotide phosphodiesterase of the bovine retina: activity, subcellular distribution, and kinetic parameters, J. Neurochem. 22:93, 1974.
3. Chader, G. J., Bensinger, R. E., Johnson, M., and Fletcher, R. T.: Phosphodiesterase: an important role in cyclic nucleotide regulation in the retina, Exp. Eye Res. 17:483, 1973.
4. Farber, D. B., and Lolley, R. N.: Enzymatic basis for cyclic GMP accumulation in degenerative photoreceptor cells of mouse retina, J. Cyclic Nucleotide Res. 2:139, 1976.
5. Richards, G. M., duVair, G., and Laskowski, M.: Comparison of the levels of phosphodiesterase, endonuclease, and monophosphatases in several snake venoms, Biochemistry 4:501, 1965.
6. Chader, G., Fletcher, R., Johnson, M., and Bensinger, R.: Rod outer segment phosphodiesterase: factors affecting the hydrolysis of cyclic-AMP and cyclic-GMP, Exp. Eye Res. 18:509, 1974.

The role of hemolysin in corneal infections with *Pseudomonas aeruginosa*.

MARY K. JOHNSON AND JAMES H. ALLEN.

Cultures of Pseudomonas aeruginosa *considered to be of proven virulence were found to have higher titers of extracellular hemolysin than cultures of lesser virulence. Intracorneal injection of purified hemolysin produced extensive corneal opacification with extensive leukocytic infiltration of the tissue. It is suggested that the hemolysin plays a role in the pathogenesis of* P. aeruginosa *infections by effecting lysis of host cells and/or subcellular organelles, leading to the release of enzymes destructive to corneal tissue.*

The role of various factors elaborated by *Pseudomonas aeruginosa* in the destruction of ocular tissue has been studied by several investigators. Fisher and Allen[1, 2] produced ulceration of the cornea with cell-free extracts and with partially purified protease preparations from this organism. More recently, the role of proteolytic enzymes in *Pseudomonas* ulcers has been studied by other investigators.[3, 4] The production of damage to corneal ground substance by enzymes from *Pseudomonas* was reported by Brown et al.[5] and by Gray and Kreger.[6] The possible role of *host* enzymes in tissue degradation was discussed by the latter authors and further explored by Kessler et al.,[7] who concluded that corneal destruction by *P. aeruginosa* depends not only on the protease, which rapidly destroys the cornea, but also on host-derived enzymes which are capable of degrading both collagen and proteoglycans.

In a preliminary survey in which we compared various characteristics of strains of *P. aeruginosa* of proven virulence with those of strains of undetermined virulence, we noted that the former appeared to be more hemolytic on human blood

0146-0404/78/0517-0480$00.40/0